Int J Earth Sci (Geol Rundsch) (2010) 99:1427–1436
DOI 10.1007/s00531-009-0458-9

REVIEW ARTICLE

Integrated geoelectrical survey for groundwater and shallow subsurface evaluation: case study at Siliyin spring, El-Fayoum, Egypt

Mohamed Metwaly · Gad El-Qady · Usama Massoud · Abeer El-Kenawy · Jun Matsushima · Nasser Al-Arifi

Received: 7 May 2008 / Accepted: 18 May 2009 / Published online: 5 June 2009

Abstract Siliyin spring is one of the many natural fresh water springs in the Western Desert of Egypt. It is located at the central part of El-Fayoum Delta, which is a potential place for urban developments and touristic activities. Integrated geoelectrical survey was conducted to facilitate mapping the groundwater resources and the shallow subsurface structures in the area. Twenty-eight transient electromagnetic (TEM) soundings, three vertical electrical soundings (VES) and three electrical resistivity tomography (ERT) profiles were carried out around the Siliyin spring location. The dense cultivation, the rugged topography and the existence of infra structure in the area hindered acquiring more data. The TEM data were inverted jointly with the VES and ERT, and constrained by available geological information. Based on the inversion results, a set of geoelectrical cross-sections have been constructed. The shallow sand to sandy clay layer that forms the shallow aquifer has been completely mapped underneath and around the spring area. Flowing of water from the Siliyin spring is interconnected with the lateral lithological changes from clay to sand soil. Exploration of the extension of Siliyin spring zone is recommended. The interpretation emphasizes the importance of integrating the geoelectrical survey with the available geological information to obtain useful, cheap and fast lithological and structural subsurface information.

Keywords Geoelectric · TEM · ERT · Siliyin spring · Egypt

M. Metwaly (✉) · G. El-Qady · U. Massoud
National Research Institute of Astronomy and Geophysics, Helwan, Cairo, Egypt
e-mail: mmetwaly70@yahoo.com

M. Metwaly · J. Matsushima
Geosystem Department, Graduate School of Engineering, Tokyo University, Tokyo, Japan

A. El-Kenawy
Geology Department, Faculty of Science, Zagazig University, Zagazig, Egypt

M. Metwaly
Al-Quwy'yia Community College, King Saud University, Riyadh, Saudi Arabia

N. Al-Arifi
Geology Department, College of Science, King Saud University, Riyadh, Saudi Arabia

Introduction

El-Fayoum province (Fig. 1) is one of the largest depressions in the western desert of Egypt. It is located 90 km South-West of Cairo and covers a total area of about 6,068 km^2. El-Fayoum is an oasis, surrounded by desert from all directions except form the south-east direction where it is connected to the Nile Valley by a Canal called Bahr Youssef. The basin formed initially along the Tethyan margin in Jurassic time. Its current shape comes from subsidence that terminated in late Eocene time. This depression is a closed basin with an altitude ranging from 24 m above sea level to 53 m below sea level on the beds of Lake Qarun, which lies in the north. Natural breaks in the level of the River Nile have caused repeated flooding of the basin.

Siliyin spring (Ain El-Siliyin) is one of the oldest natural fresh water springs in El-Fayoum depression. It is located in the heart of El-Fayoum Delta between Lake Qarun and El-Fayoum town (Fig. 1) and away from Lake Qarun by about 13 km. The name (Siliyin) refers to the abundance of

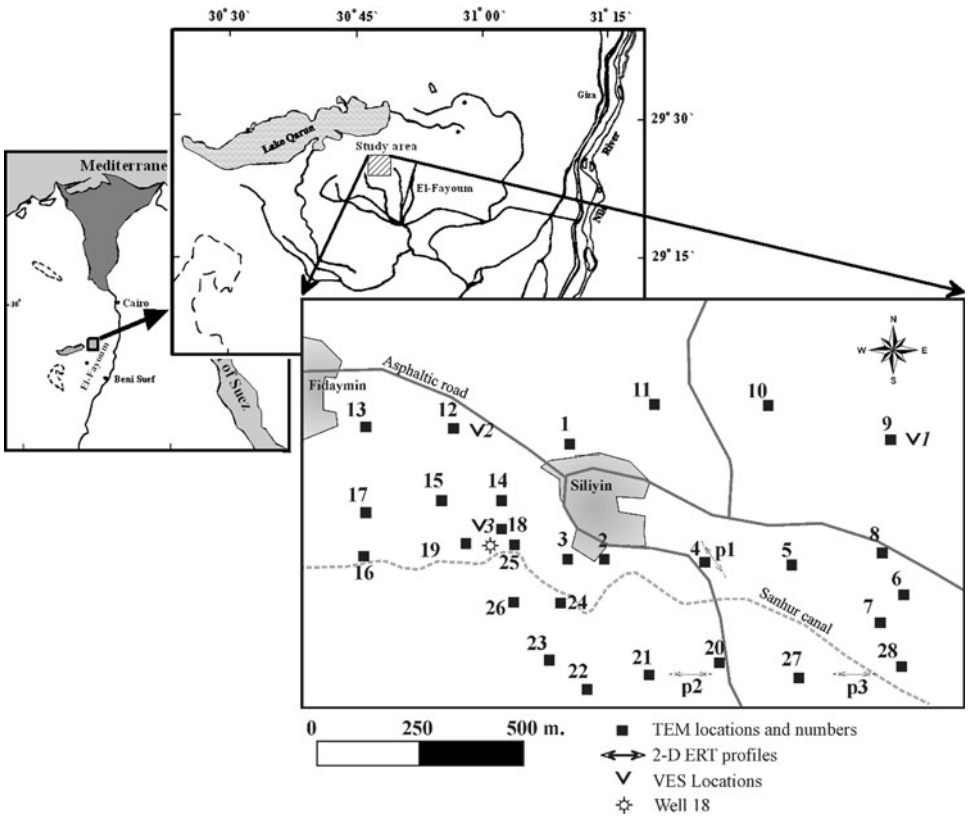

Fig. 1 Location map of the study area showing the positions of the measured stations, well and profiles

Suyul (torrential streams) in the area. In the Arabic language, Siliyin means 'two streams'. The area is very promising for touristic activities as it is surrounded by engulf trees at different step stages, many waterfalls, and fresh water springs. The water at Siliyin spring is flowing up with substantial rate. This water has temperature of about 23.5°C at the ground surface.

To understand the source and the nature of Siliyin water spring and the subsurface geologic setting control this important water source, the current surface geophysical surveys have been performed. Hence, the aim of this work is to map the extent of the groundwater-bearing layer using TEM, VES, and ERT measurements in order to evaluate of the freshwater resources in the study area. The results of this study will definitely help any future plans to develop the study site.

Geological context

Generally, the geological setting of El-Fayoum has been addressed in details by many authors (Said 1962; Tamer 1968; Swedan 1986). However, in the following section, we will describe briefly the subsurface geology that may help for geophysical data interpretation in the study area.

The subsurface geological section in the study area starts by Quaternary rocks, which have a very wide distribution over El-Fayoum area (Fig. 2). The alluvial sediments of the Nile basin were deposited directly over the Plio-pleistocene sediments. These alluvial sediments are extending to depth of about 60 m and composed of sands and gravels of variable sizes intercalated with silt and clay contents (Tamer 1968). The Lacustrine deposits of Pleistocene are composed of claystone, gypsum, and calcareous materials intercalated with ferruginous sandy silt. They are prevailed in the area and extend to the south of Lake Qarun. In El-Fayoum depression, Quaternary sediments are directly overlying the limestone deposits of Eocene age, where the latter extends to a greater depth. The thickness of the Quaternary sediments varies from place to place. It reaches to about 47 m at the center of the depression (Fig. 3) and varies according to the configuration of the underlying limestone rocks. The Quaternary sediments resulted from the seasonal flood of the River Nile over the area during the Pleistocene and Holocene times. The sand and gravel sediments accumulated form the water-bearing material of the Quaternary aquifer, while silt and clay are considered the water-confining materials. Structurally, El-Fayoum depression has been affected by several distortion lines (faults, breaks, etc.) in addition to some folds. The

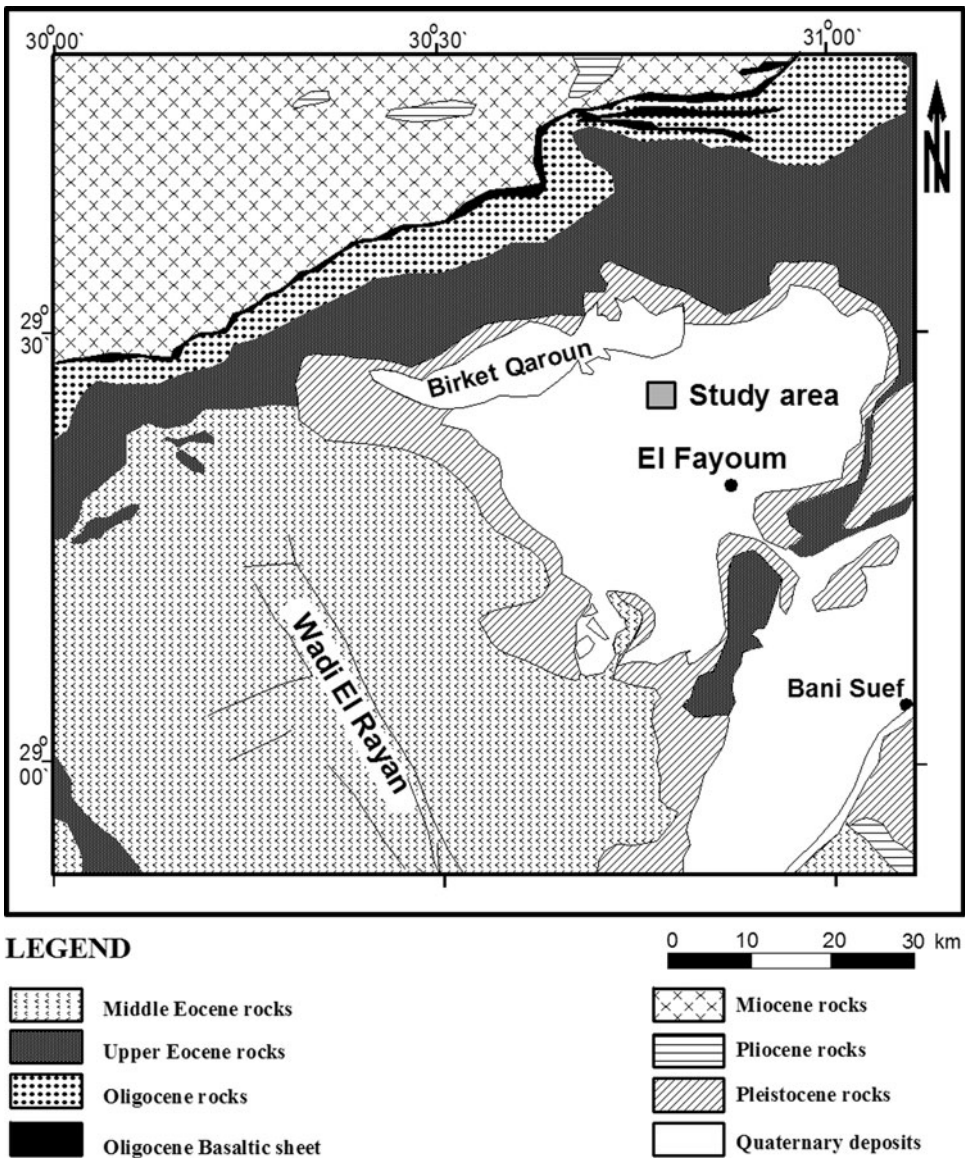

Fig. 2 Surface geological map of El-Fayoum depression including the study area (modified after Beadnell 1905)

distortion lines are particularly dominant at the edges of the depression with N-S and NW-SE striking directions. These structural features in addition to the weathering conditions have contributed to the formation of El-Fayoum depressions.

Hydrogeological context

Generally, the groundwater in El-Fayoum Delta can be obtained from different water-bearing zones. We will emphasize on the shallow water-bearing formations of Quaternary and Eocene directly related to the object of this study.

Quaternary water-bearing formation

The Quaternary water-bearing formations cover most of El-Fayoum depression and extend in the subsurface with variable thicknesses depending on the shape of the underlying Eocene limestone. The maximum thickness of the shallow aquifer is about 34 m close to Siliyin area (Fig. 3). This shallow aquifer is considered as a confined aquifer because it is capped with clay sediments (confining layer). The groundwater in this confined aquifer is estimated to be under pressure. At some localities, groundwater from Quaternary deposits flows as natural springs, for example, Ain El-Siliyin, Ain El-Shaer, and Ain Fidaymin. The depth to water, as encountered from shallow wells in and around

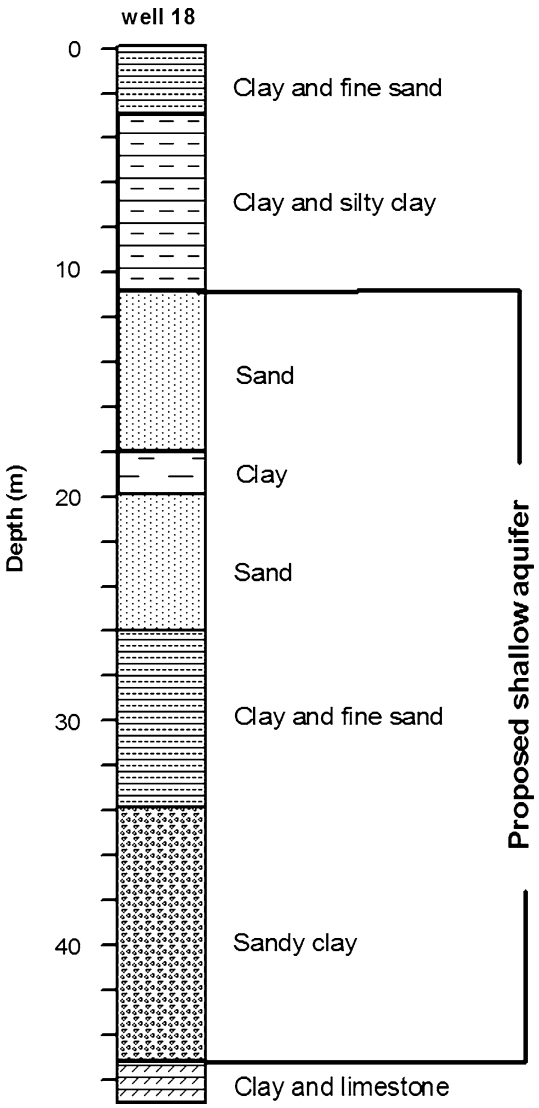

Fig. 3 Lithological succession as deduced from wells 18 with the location of the proposed shallow aquifer, for the well location refer to Fig. 1

the study area, varies from few centimeters to 5 m. Locally at Siliyin area, it is typically 4 m below ground level (Fig. 4). The sources recharging the Quaternary aquifer include the irrigation water, surface channels, water flowing from the River Nile through Hawara depression and the nourishing from the underlying fractured limestone aquifers through hydraulic connection.

Eocene water-bearing formation

These sediments are represented by the structural limestone plateau that surrounds El-Fayoum, Rayan, Nile River, and Hawara depressions. The water-bearing deposits of the Eocene age is a fractured limestone underlying the Quaternary deposits and extending to a depth of about 600 m. The feeding of this aquifer comes from the Quaternary aquifers and through the hydraulic connection to the underlying Cretaceous aquifers.

The water of Siliyin spring is alkaline (pH = 7.3), where carbonates constitute about 70% (410 mg/l) of the total dissolved solids in the water as shown in Table 1. Moreover, Siliyin groundwater contains some traces of titanium, vanadium, iron, and aluminum, which are considered as natural therapeutic substances used especially for treatment the high gastric acidity problems. Nearby Siliyin well, a pumping test was conducted. The groundwater electrical conductivity (EC at 25°C) was measured for some water samples and has ranged from 2.1 to 2.2 mS/cm at the beginning of the pumping and after 4 h, respectively (FWMP 1999).

Geophysical data

The geophysical study described in this work is based mainly on geoelectrical surveys. Indeed the geoelectrical techniques are essentially concerned by measuring the electrical conductivity of the subsurface materials, which preferentially provides information on the different geological layers, structures and sometimes the conditions of the associated groundwater (Van Overmeeren 1989; Stewart 1982; Repsold 1990; El-Waheidi et al. 1992; Nowroozi et al. 1999; Meju 2005). In general, there is no single geoelectrical technique being able to provide unique information about the subsurface conditions. Meanwhile, the success of each geoelectrical technique depends to large extent on the site conditions, the possible resolution of the utilized array and the impact of the 3D subsurface structure on the acquired geophysical data. The integration of more than one geophysical technique will presumably provides consistent data sets that reduce the uncertainty of the interpreted models. As applied in this work, we have integrated the transient electromagnetic (TEM) technique with both vertical electrical sounding (VES) and electrical resistivity tomography (ERT), in order to obtain robust subsurface models.

VES data

In this study, the VES data were collected by SYSCAL R2 resistivity meter, where the conventional Schlumberger configuration with current electrode separation (AB) varying from 2 up to 400 m has been employed. The recording system was adopted to automatically adjust the input current at a maximum voltage of 200 V. The study area was densely cultivated land with locally irregular

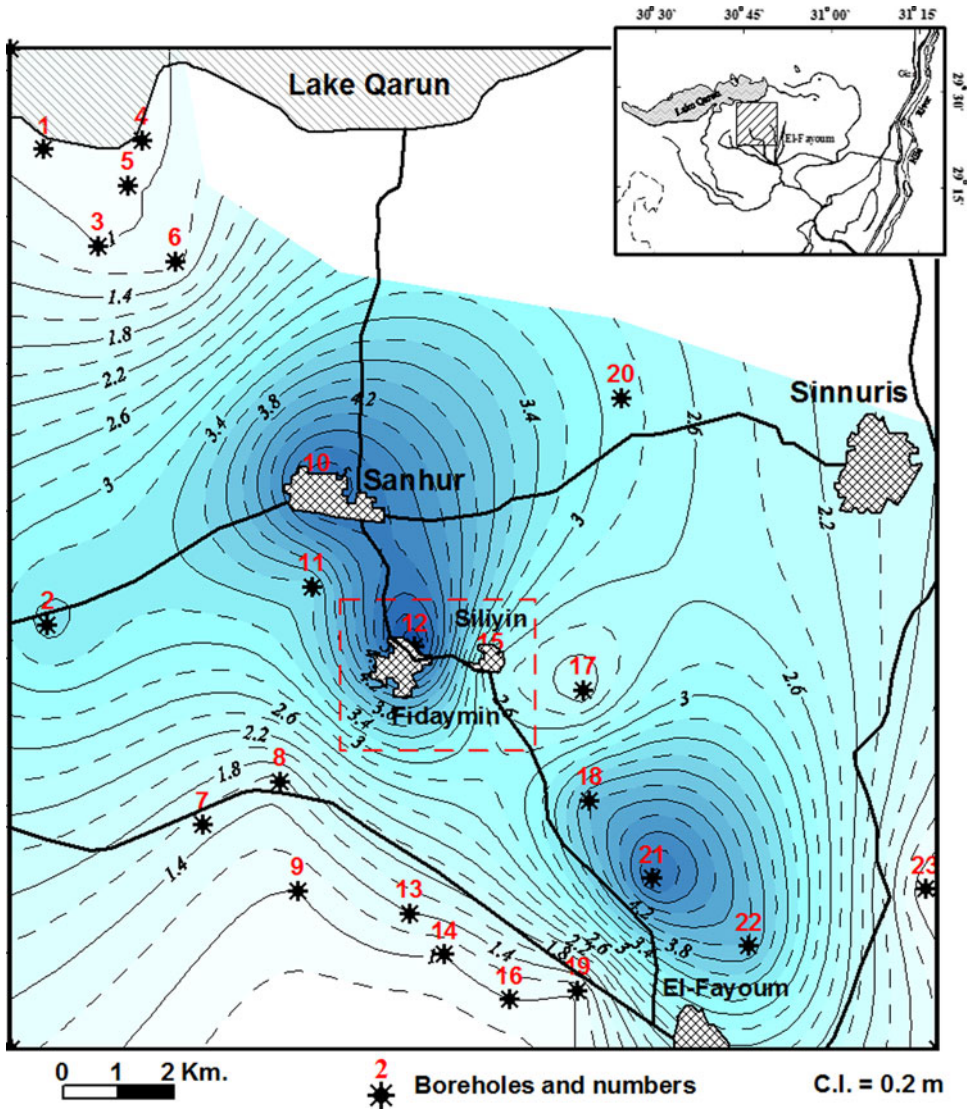

Fig. 4 Depth to water in the area around Siliyin spring at El-Fayoum depression, the detailed studied area is marked by *red dashed line*

Table 1 Chemical composition of Siliyin spring's water

Chemical element	Percentage (mg/l)
Calcium	154
Sodium	45
Magnesium	24
Potassium	4
Bicarbonates	23
Nitrates	1.3
Sulfates	87
Chlorides	72
pH	7.3

topographic features and farm's fences. Therefore, VES data could be acquired at three sites only (Fig. 1) and have been used to perform a combined inversion with the near TEM data sets. The acceptable 1D starting model can be used in the inversion of the remainder TEM data sets as there are no specific lithological logs available (Fig. 5).

TEM data

The TEM method is an electromagnetic induction technique for which the response of the earth to an electromagnetic impulse is measured in the time domain. A thorough discussion of the TEM method and the interpretation of TEM data can be found in Nabighian and Macnae (1991). Recently, the TEM method has been extensively used in hydrogeophysical surveys, including the search for groundwater resources (McNeill 1990; Danielsen et al. 2003; Nielsen et al. 2006; Cosentino et al. 2007). The technique is considered an effective tool for characterizing the subsurface based on the variations in the electrical conductivity (Meju 2005).

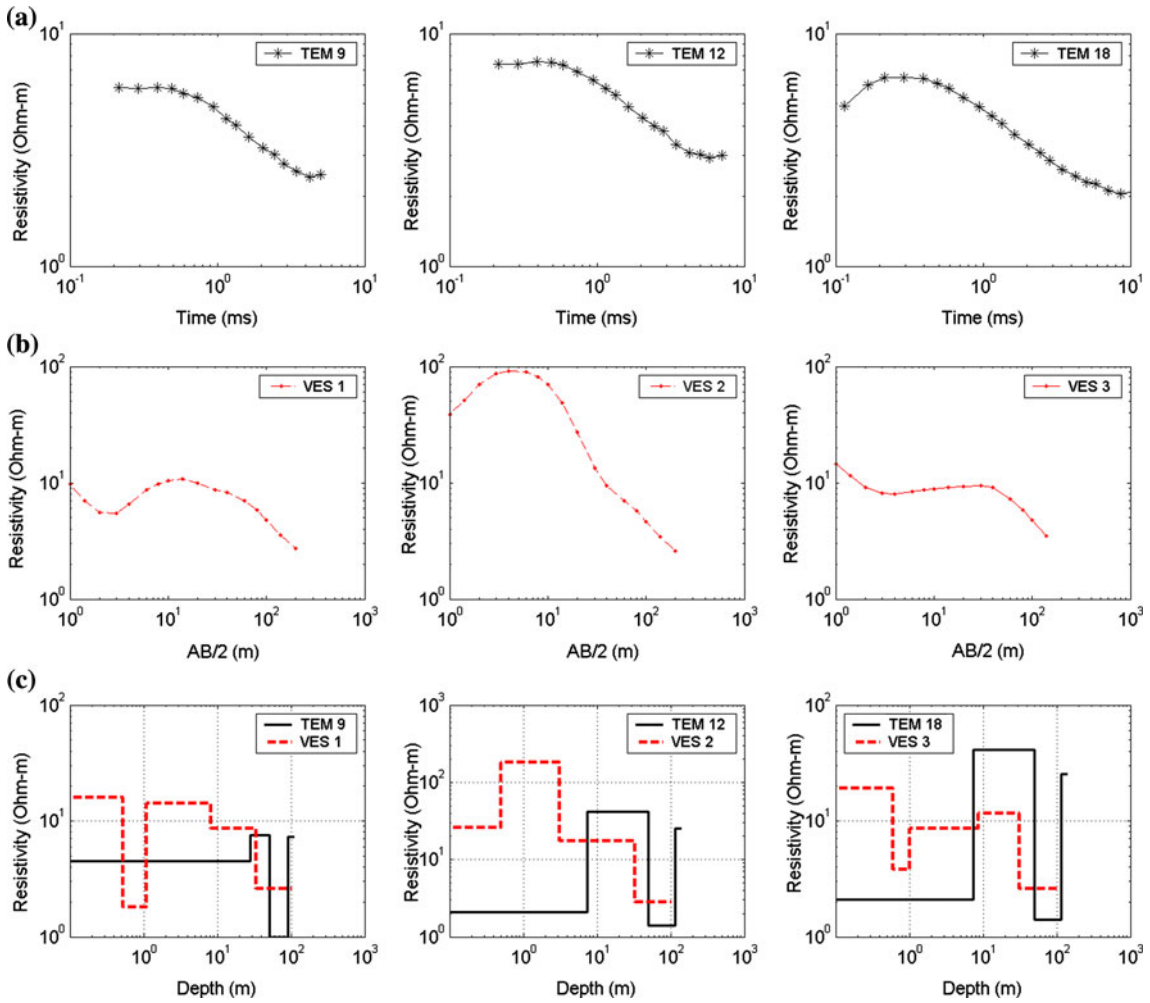

Fig. 5 Examples of TEM and VES data processing and the resulted models at Siliyin area. **a** Example of TEM data, **b** example of VES data, **c** example of TEM- and VES-layered models

TEM survey was conducted in the studied area using *SiroTEM MK3* system. The field data have been recorded at 28 stations shown in Fig. 1. Some local areas are sparsely covered with TEM stations due to the rugged topography, dense cultivations and subsurface infrastructures (metallic irrigation pipes). Therefore, the distances between the measuring stations were ranging from 50 to 500 m. A common coincident squared loop configuration with a loop side length of 25 m has been employed in this work. The data have been collected using composite mode, whereas the measurement times ranged from 0.11 to 23.84 ms after the primary transmitter current is turned-off through 25 time gates. The receiver coil measures the time rate change of the magnetic field as a function of time (dB/dt) during the transient. Each measurement has been stacked 28 times for reducing the noise effect of the recorded data. An example of measured real signals and noise is shown in Fig. 6. The signal response is extensively strong and competent, whereas the background noise is assorted in character. The latest time of the recorded signal can be distorted by the background noise, which can be easily treated using editing function before further processing of the data.

ERT data

Electrical resistivity tomography is a well-established technique for both 2D and 3D subsurface electrical imaging (Barker and Moore 1998; Ramirez and Daily 2001; Kemna et al. 2002; Daily et al. 2004). The measurements are normally carried out using computer-controlled system with large number of electrodes laid out along straight lines with constant spacing. In the current work, we carried

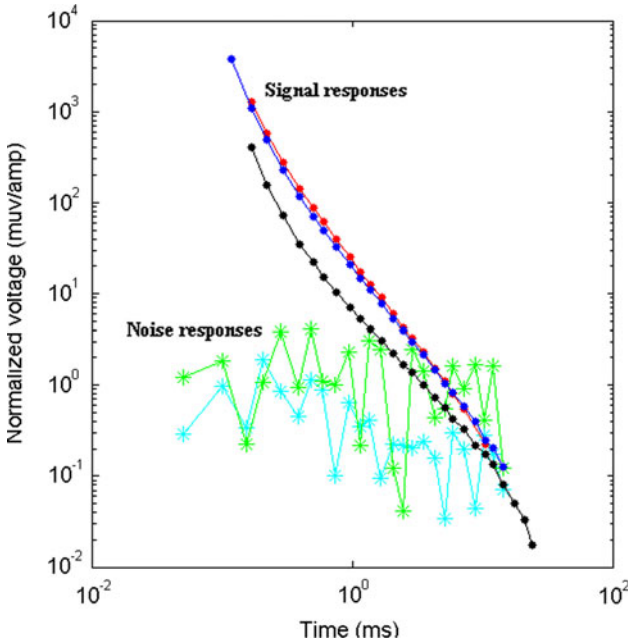

Fig. 6 Examples of the TEM recorded signals and noise at Siliyin area

out 2D ERT utilizing 30–48 electrodes connected to the SYSCAL R2 recording system functioned with the Dipole–Dipole electrode configuration. The dipole–dipole array has been chosen because it is more sensitive to horizontal resistivity changes rather than the vertical resistivity changes. Moreover, it has better horizontal data coverage than other electrode arrays (Loke 1998). The electrode spacing was fixed to be 5 m and (n) was changed from 1 up to 7 times of the dipole length to obtain the maximum depth of investigation and lateral resolution. Three ERT profiles have been acquired close to and in between the TEM stations at the possible locations to get detailed information about the shallow subsurface. Before current injection, the electrode contact resistance values had been checked and assured to be as low as possible. The voltage value had been set at 200 V, while the injected current values were automatically adjusted by the recording system. Then the measurements were stacked at least three times for each point along the profile to enhance data quality. Standard deviation is used for evaluating the statistical dispersion of recorded resistivity data from their arithmetic mean.

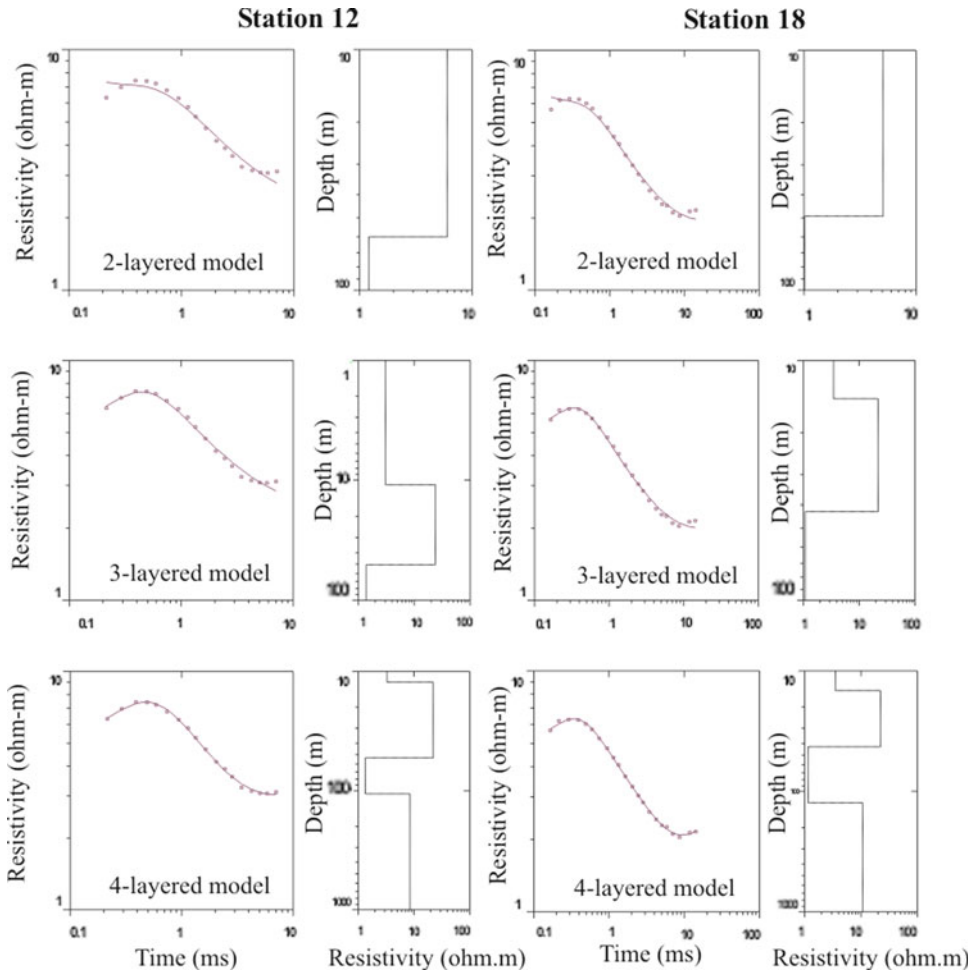

Fig. 7 Apparent resistivity data curves and the corresponding 2-, 3-, and 4-layered models

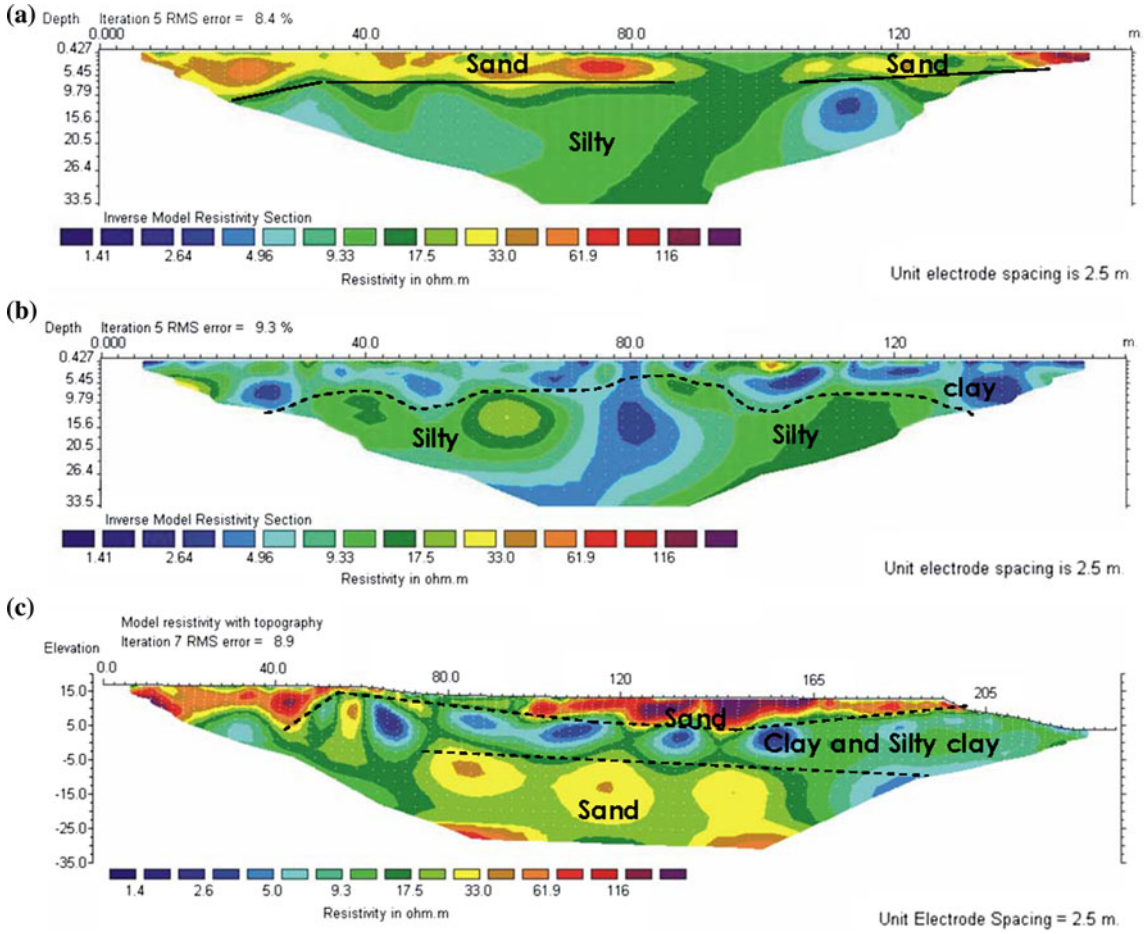

Fig. 8 Inverted ERT profiles at the study area, **a** for profile-1, **b** for profile-2, and **c** for profile-3

Data processing and inversion

The electrical resistivity and TEM methods are complementary in many ways making them ideal partners for combined inversion process (Yang et al. 1999; Meju 2005). Although both methods measure electrical conductivity or resistivity of the subsurface, they sample different subsurface volumes and therefore they have different subsurface sensitivities.

The VES data were first inverted individually in terms of 1D resistivity-depth models based on the available geological information using IPI2Win software (Fig. 5b, c). Then the resultant models have been used as starting models in the inversion process of the nearby TEM data sets. A simple comparison demonstrates the behavior of both VES and TEM models (red dashed and black solid lines in Fig. 5c, respectively). At the shallow depth ($\leq$10 m.), the inversion process is mainly constrained by the VES data only. The TEM data at that depth provides only very weak constraints due to the relatively late times of the first TEM records. In contrast, the VES data gives more details about the resistivity variations at that shallow depth due to the dense suites of resistivity measurements using relatively short electrode separations. At greater depth, the inversion process is constrained mainly by the TEM data, which provides a reasonable resolution at that depth. At the intermediate depths the models have been obtained from the contribution of both (VES and TEM) data sets.

Due to the limited number of VES stations that can be used in setting the robust starting model for TEM data inversion, there is strong need for selecting the optimum starting model in areas have neither sufficient well information nor VES data. In this context, several criteria have been tested including different number of layers and thicknesses during the preliminary TEM data processing. The robust model was the one that provides minimum error, maximum fit and best matching with the other data set as well as the available borehole's information (Fig. 7). A primary simplified two-layer model has poorly fitted the

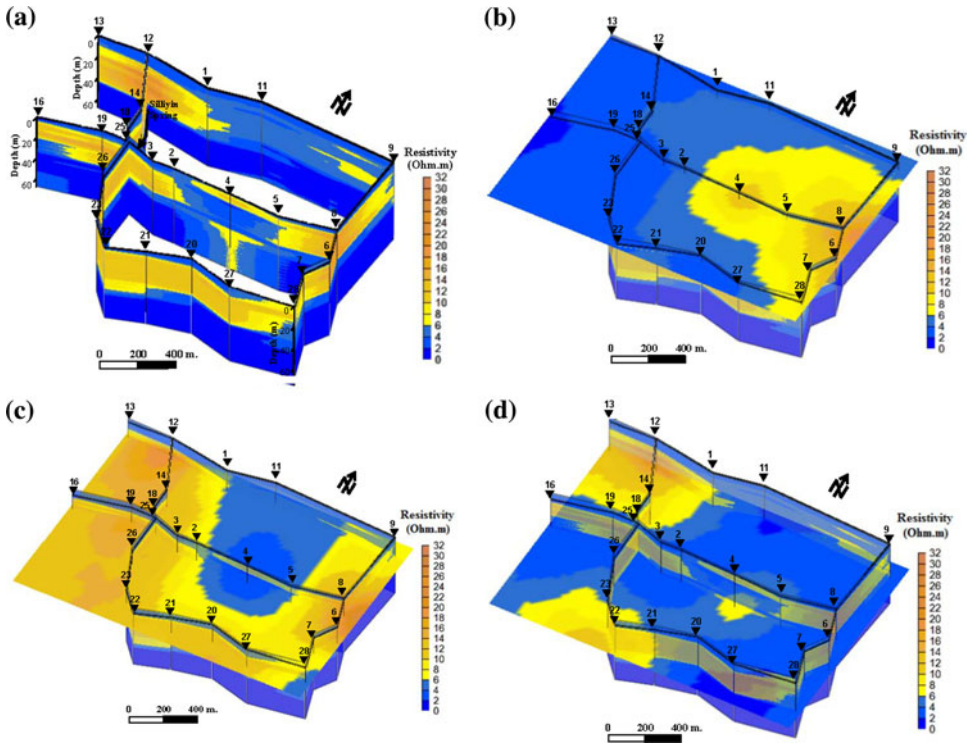

Fig. 9 Panel diagrams represent the 3D view of the resistivity cross-sections along the studied area, for the stations location refer to Fig. 1. **a** Fence diagrams, **b** resistivity slice at depth about 10 m from the surface, **c** resistivity slice at depth about −10 m from the surface and **d** resistivity slice at depth about −30 m from the surface

measured data especially at the early and late times of the TEM curve. The degree of fitting has improved thoroughly with increasing the number of layers to four (Fig. 7).

The ERT data was inverted in 2D scheme by using an iterative smoothness-constrained least squares inversion, Res2Dinv (Loke 1998; Barker and Moore 1998). The robust inversion process of ERT profiles attained the convergence with RMS error varying from 8 to 10%. There were no much differences in the inverted models for the last three iterations, so that we accepted the model of lower RMS error. Generally, the inverted resistivity model along profile 3 (Fig. 8) shows that the study area is characterized by relatively low resistivity background ranging from 5 to 17 Ωm. These low resistivity values refer to the dominant clay and silty clay sediments at the surface as well as to the shallow saturated sand to silty clay aquifer (Fig. 8). Locally at the surface, relatively high resistivity zones (33–120 Ωm) could be identified, which might be attributed to the prevalence of dry soils at the surface.

Discussion and conclusion

The final output of the integrated interpretation of the electrical resistivity and TEM data are set of multi-layered models, each of them satisfies the response of the comparable two data sets (VES and/or TEM) and describes the electrical properties of the shallow subsurface medium. These models have been used for preparing a fence diagram and isopach maps in the study area (Fig. 9). Powerful geostatistical gridding (kriging) method has been applied to smoothly interpolate the measured data. Linear color scale has been used to visualize the limited resistivity range (1–32 Ωm).

The top layer has a maximum depth of 11 m and relatively low resistivity values (<6Ωm), which is most likely due to moist agricultural clay soil (Figs. 5, 8b, 9a). However, toward the center and the southeastern part of the study area, this layer thins and completely vanishes under station (28) as shown in Figs. 8, 9a, b). The same layer shows relatively high resistivity values (>6 Ωm) due to the lithological variation from agricultural clay soil to dry sandy soil (Fig. 9b). Along the 2D resistivity profiles (p1 and p3) and station (4), the first sandy layer is separated from the underlying sand aquifer by a clay to silty clay layer (Figs. 8a, 9a, c). This first low resistivity clay layer appears under thin sand layer and acts as a cap for the shallow aquifer.

The second major layer in the study area is characterized by high resistivity values (>6 Ωm) and is extending to depth of about 45 m (Figs. 5, 8, 9c). This layer is composed mainly of sandy sediments and forms the shallow confined Quaternary aquifer in the study area (Fig. 3). At some localities, the second layer exhibits a relatively low resistivity particularly at the central and northern parts of the study area (Fig. 9a, c). This feature may be attributed to the tectonic and/or lateral changes of the depositional

environment, which has changed the sedimentary facies from sandy to clayey materials (Fig. 9, stations 11, and 4).

The third layer is characterized by low resistivity values and extends to the base of the sections. It is most likely composed of clayey sediments as it shows low resistivity values (<6 Ωm) as shown in Fig. 3. However at station 4 (Fig. 9a, d), which is contiguous with the Siliyin spring, this layer shows a high resistivity value (>6 Ωm) surrounded by low resistivity values. This feature did not show up on profile (P1, Fig. 8a), as it exists beyond the maximum depth of penetration reached by the resistivity data.

Siliyin spring is located between stations 3 and 25 (Fig. 9a) whereas the shallow aquifer sand layer has considerable lateral changes to clay and sand clay toward the eastern direction under stations 2 and 4. These lateral changes can be attributed to structural or lithofacies changes in such a way that makes the shallow aquifer connected to the deep Eocene limestone aquifer. Consequently, the shallow aquifer is continuously charged from the deeper one and the spring water is following naturally throughout the weak points of the clay cap layer.

From the obtained subsurface geophysical results, it is recommended that any proposed projects for future developments around the Siliyin spring should consider the fact that the shallow sandy aquifer has a reasonable thickness and is connected to the deep aquifer. These conditions could be ideally observed around the location of stations 2 and 5 (Fig. 9a).

Acknowledgments The work of the first author is partially supported by the Japanese Society for the Promotion of Science (JSPS).

References

Barker RD, Moore J (1998) The application of time-lapse electrical tomography in groundwater studies. Lead Edge (Tulsa Okla) 17:1454–1458. doi:10.1190/1.1437878

Beadnell HJL (1905) The topography and geology of the Fayum province of Egypt. Egyptian Survey Department, Cairo, p 101

Cosentino P, Capizzi P, Fiandaca G, Martorana R, Messina P, Pellerito S (2007) Study and monitoring of salt water intrusion in the coastal area between Mazara del Vallo and Marsala (South-Western Sicily). In: Rossi G, Vega T, Bonaccorso B (eds) Methods and tools for drought analysis and management. Series: water science and technology library. Springer, Dordrecht. ISBN 978-1-4020-5923-0

Daily W, Ramirez A, Binley A, LeBrecque D (2004) The meter reader—electrical resistance tomography. Lead Edge (Tulsa Okla) 23:438–442. doi:10.1190/1.1729225

Danielsen JE, Auken E, Jorgensen F, Sondergaard V, Sorensen K (2003) The application of TEM in hydrogeophysical surveys. J Appl Geophys 53:181–198. doi:10.1016/j.jappgeo.2003.08.004

El-Waheidi MM, Merlanti F, Pavan M (1992) Geoelectrical resistivity survey of the central part of Azraq basin (Jordan) for identifying saltwater/freshwater interface. J Appl Geophys 29:125–133. doi:10.1016/0926-9851(92)90003-4

FWMP (1999) Fayoum water management project II "Salinisation monitoring of Lake Qarun between 1901 and 1998". Technical Report No. 55, p 16, XXII

Kemna A, Vanderborght J, Kulessa B, Vereecken H (2002) Imaging and characterisation of subsurface solute transport using electrical resistivity tomography (ERT) and equivalent transport models. J Hydrol (Amst) 267:125–146. doi:10.1016/S0022-1694(02)00145-2

Loke MH (1998) RES2DINV, rapid 2D resistivity and IP inversion using least-squares methods. User manual, Austin Tex., Advanced Geosciences, Inc., Seattle, p 66

McNeill JD (1990) Use of electromagnetic methods for groundwater studies. In: Ward SH (ed) Geotechnical and environmental geophysics, 02. Society of Exploration Geophysicists, pp 191–218

Meju M (2005) Simple relative space–time scaling of electrical and electromagnetic depth sounding arrays: implications for electrical static shift removal and joint DC-TEM data inversion with the most-squares criterion. Geophys Prospect 53:1–17. doi:10.1111/j.1365-2478.2005.00483.x

Nabighian MN, Macnae JC (1991) Time domain electromagnetic prospecting methods. In: Nabighian MN (eds) Electromagnetic methods in applied geophysics-applications, Volume 2, Part A, vol 3. Society of Exploration Geophysics, Investigations in Geophysics, p 520

Nielsen L, Jorgensen N, Gelting P (2006) Mapping of the freshwater lens in a coastal aquifer on the Keta Barrier (Ghana) by transient electromagnetic soundings. J Appl Geophys 62:1–15. doi:10.1016/j.jappgeo.2006.07.002

Nowroozi AA, Horrocks SB, Henderson P (1999) Saltwater intrusion into the freshwater aquifer in the eastern shore of Virginia; a reconnaissance electrical resistivity survey. J Appl Geophys 42:1–22. doi:10.1016/S0926-9851(99)00004-X

Ramirez A, Daily W (2001) Electrical imaging at the large block test–Yucca Mountain, Nevada. J Appl Geophys 46:85–100. doi:10.1016/S0926-9851(00)00042-2

Repsold H (1990) Geoelektrische Untersuchungen zur Bestimmung der Süßwasser/Salzwasser-Grenze im Gebiet zwischen Cuxhaven und Stade. Geologisches Jahrbuch C56:3–37

Said R (1962) The geology of Egypt. Elsevier, Amsterdam, p 377

Stewart MT (1982) Evaluation of electromagnetic methods for rapid mapping of salt water interfaces in coastal aquifers. Ground Water 20:538–545. doi:10.1111/j.1745-6584.1982.tb01367.x

Swedan AH (1986) Contributions to the geology of Fayoum area. PhD Thesis, Faculty of Science, Cairo University

Tamer A (1968) Subsurface geology of the Fayoum Region. MSc, Faculty of Science, Alexandria University, Egypt

Van Overmeeren R (1989) Aquifer boundaries explored by geoelectrical measurements in the coastal plain of Yemen, A case of equivalence. Geophysics 54:38–48. doi:10.1190/1.1442575

Yang C, Tongz L, Huang C (1999) Combined application of dc and TEM to sea-water intrusion mapping. Geophysics 64:417–425. doi:10.1190/1.1444546